



## Research Article

# Long Noncoding RNA LEMD1-AS1 Increases LEMD1 Expression and Activates PI3K-AKT Pathway to Promote Metastasis in Oral Squamous Cell Carcinoma

Zaiye Li <sup>1,2,3,4</sup> Jie Wang,<sup>5</sup> Jianjun Wu,<sup>1,2,3</sup> Ning Li,<sup>1,2,3</sup> and Canhua Jiang <sup>1,2,3</sup>

<sup>1</sup>Department of Oral and Maxillofacial Surgery, Center of Stomatology, Xiangya Hospital, Central South University, Changsha, China

<sup>2</sup>Research Center of Oral and Maxillofacial Tumor, Xiangya Hospital, Central South University, Changsha, China

<sup>3</sup>Institute of Oral Cancer and Precancerous Lesions, Central South University, Changsha, China

<sup>4</sup>State Key Laboratory of Oral Diseases, National Clinical Research Center for Oral Diseases, Chinese Academy of Medical Sciences Research Unit of Oral Carcinogenesis and Management, West China Hospital of Stomatology, Sichuan University, Chengdu, Sichuan 610041, China

<sup>5</sup>Department of Immunology, Xiangya School of Medicine, Central South University, Changsha, China

Correspondence should be addressed to Canhua Jiang; canhuaj@csu.edu.cn

Received 20 May 2022; Accepted 7 July 2022; Published 9 August 2022

Academic Editor: Wei Han

Copyright © 2022 Zaiye Li et al. This is an open access article distributed under the Creative Commons Attribution License, which permits unrestricted use, distribution, and reproduction in any medium, provided the original work is properly cited.

**Background.** The survival rate of oral squamous cell carcinoma (OSCC) is only 50% due to a high incidence of metastasis. Long noncoding RNAs (lncRNAs) play a crucial role in OSCC genesis and progression, although their potential role in the metastasis of OSCC remains unclear. **Methods.** The transcriptome of 5 metastatic and 5 nonmetastatic OSCC samples were assessed by RNA sequencing. The biological functions and regulatory mechanisms of LEMD1-AS1 in OSCC were explored by in vitro and in vivo assays. **Results.** We identified 487 differentially expressed mRNAs (DEmRNAs) and 1507 differentially expressed lncRNAs (DElncRNAs) in OSCC with cervical lymph node (LN) metastasis relative to the nonmetastatic samples. In addition, both LEMD1-AS1 and its cognate LEMD1 were up-regulated in metastatic OSCC compared to nonmetastatic OSCC. Gain-of-function, loss-of-function, and rescue experiments indicated that LEMD1-AS1 upregulated LEMD1 to increase OSCC migration and invasion in vitro and in vivo. Mechanistically, LEMD1-AS1 stabilized LEMD1 and increased its mRNA and protein levels, and consequently activated the PI3K-AKT signaling pathway to facilitate OSCC metastasis. **Conclusions.** We established the lncRNA-mRNA landscape of metastatic OSCC, which indicated that LEMD1-AS1 enhanced OSCC metastasis by stabilizing its antisense transcript LEMD1. Thus, LEMD1-AS1 is a potential biomarker for predicting metastasis, as well as a therapeutic target of OSCC.

## 1. Background

Oral squamous cell carcinoma (OSCC) is one of the most commonly diagnosed malignancies worldwide [1–3] and is characterized by a high incidence of local invasion and cervical lymph node (LN) metastasis. Despite recent advances in surgery, chemoradiotherapy, and other targeted therapies, the overall survival of OSCC patients is still only 50% due to the high metastasis rates [4, 5]. Therefore, it is essential to

identify the underlying mechanisms of OSCC metastasis in order to develop novel effective therapies.

Long noncoding RNAs (lncRNAs) are noncoding transcripts more than 200 nucleotides in length [6, 7] and are classified into the antisense, intronic, bidirectional, intergenic, and overlapping types. lncRNAs regulate gene expression via chromatin modification, miRNA quenching, direct modulation of mRNA stability, transcription, and translation, as well as protein stability control [8, 9], and are involved in tumor

initiation and progression. The antisense lncRNAs account for approximately 50–70% of all lncRNAs and can exert their function through *cis*- or *trans*-mechanisms [10]. The *cis*-acting antisense lncRNAs bind to genes in their vicinity, while the *trans*-lncRNAs modulate more distant genes on the same or even on different chromosomes. Furthermore, *cis*-antisense lncRNAs modulate gene expression at the pretranscriptional, transcriptional, and posttranscriptional levels through DNA–lncRNA, lncRNA–RNA, or protein–lncRNA interactions. lncRNA–RNA interactions in particular are common during cancer initiation and progression and involve hybridization of the sense and antisense sequences into RNA duplexes that regulate the posttranscriptional outcome. Zhao et al. reported that MACC1-AS1 promoted gastric cancer cell metabolic plasticity by stabilizing MACC1 mRNA [11]. In addition, lncRNA PXN-AS1-L acts as an oncogene in non-small-cell lung cancer (NSCLC) by increasing PXN expression [12]. Yuan et al. found that MUC5B-AS1 promoted lung adenocarcinoma metastasis by forming RNA–RNA duplex with MUC5B. However, little is known regarding the function of antisense lncRNAs in metastatic OSCC.

To this end, we performed next-generation sequencing analysis of human OSCC tissues in order to map the differentially expressed RNAs and establish a lncRNA–mRNA interaction network. Accordingly, we identified lncRNA LEMD1-AS1 and its target gene LEMD1, which acts as an oncogene in multiple cancers, and analyzed their biological role in OSCC via functional assays. Our findings provide new insights into OSCC metastasis and identify a novel biomarker for prognostic prediction and targeted therapy.

## 2. Results

**2.1. Overview of RNA Sequencing Data.** All raw data had been uploaded in GEO database (GSE145272, <https://www.ncbi.nlm.nih.gov/geo/query/acc.cgi?acc=GSE145272>). A total of 487 differentially expressed mRNAs (DEmRNAs) (319 upregulated and 168 downregulated) and 1507 differentially expressed lncRNAs (DELncRNAs) (971 upregulated and 536 downregulated) were identified in RNA-seq data using  $|\log_2 \text{fold change (FC)}| > 1.0$  and  $P \text{ value} < 0.05$  as the thresholds (Figure 1). The functional enrichment analysis (Additional Figure 1A) showed that 487 DEmRNAs were enriched in 520 biological process (BP), 13 cellular component (CC), and 21 molecular function (MF) terms, including cell–cell adhesion, receptor complex, channel complex, channel activity, and receptor activity. KEGG pathway analysis (Additional Figure 1B) indicated enrichment of 243 pathways, including the cAMP signaling pathway, calcium signal pathway, cytokine–cytokine receptor interaction, and cell adhesion molecules (CAMs).

**2.2. DELncRNA–DEmRNA Interaction Network.** Potential interactions between the DELncRNAs and DEmRNAs were predicted using the LncTar software and correlated via R software. The interacting pairs were screened using  $\text{cor} \neq 0$  and  $P \text{ value} < 0.05$  as the thresholds. As shown in Additional Figure 2, 132 *cis*-regulation pairs and 165994 *trans*-regulation pairs were identified.

**2.3. Validation of Dysregulated RNAs.** To validate the RNA-seq data, we randomly selected five DERNAs (LEMD1-AS1, LEMD1, TBILA, LINC01133, and PURPL) from the top 50 DERNAs identified in 10 samples by qPCR. LEMD1-AS1, LEMD1, TBILA, and LINC01133 were significantly upregulated in metastatic versus nonmetastatic OSCC while PURPL was downregulated in the former (Figure 2).

**2.4. LEMD1-AS1 and LEMD1 Are Overexpressed in Human OSCC Tissues and Cell Lines.** Since both LEMD1-AS1 and LEMD1 were upregulated in the metastatic OSCC samples relative to the nonmetastatic samples, we hypothesized that LEMD1-AS1 promotes OSCC metastasis by upregulating its predicted target LEMD1. To confirm our hypothesis, we detected the expression levels of both in additional OSCC samples by qRT-PCR. Consistent with the bioinformatics results, the metastatic tumors expressed higher levels of both LEMD1-AS1 and LEMD1, which showed a significant positive correlation (Figure 2(f)). In addition, the metastatic OSCC cell lines UM1, OSC19, and CAL27 showed significantly higher LEMD1-AS1 levels compared to the nonmetastatic UM2 and OSC3 cells (Additional Figure 3). Taken together, the LEMD1-AS1 and LEMD1 interaction is prometastatic in OSCC.

**2.5. LEMD1-AS1 Promoted Migration of OSCC Cells via LEMD1.** FISH assay showed that LEMD1-AS1 was mainly localized in the cytoplasm of OSCC cells, and minimal signals were observed in the nucleus (Additional Figure 4). To further analyze the biological role of LEMD1-AS1 in OSCC cells, we knocked down its expression in the OSC19 and CAL27 cells using the smart silencer (Additional Figure 5A), and ectopically expressed it in the UM2 and OSC3 cells (Additional Figure 5B). The cells overexpressing LEMD1-AS1 had higher levels of LEMD1, while LEMD1-AS1 knockdown was associated with downregulation of LEMD1 (Additional Figure 5C–D). Neither LEMD1-AS1 silencing nor overexpression had any effect on the proliferation of the OSCC cells compared to the respective controls (Additional Figure 6). However, LEMD1-AS1 overexpression in UM2 and OSC3 cells significantly increased their migration abilities *in vitro* (Figure 3), whereas LEMD1-AS1 knockdown had the opposite effect in OSC19 and CAL27 cells. Taken together, LEMD1-AS1 is a prometastatic factor in OSCC. To determine whether LEMD1-AS1 mediated its effects in OSCC via LEMD1, we knocked down the latter in cells stably overexpressing LEMD1-AS1 (Additional Figure 7). As shown in Figure 4, the knockdown of LEMD1 abrogated the effects of LEMD1-AS1 overexpression on the migration and invasion abilities of OSCC cells. Thus, LEMD1-AS1/LEMD1 interaction is crucial for OSCC progression and metastasis.

**2.6. LEMD1-AS1 Increased the Stability of LEMD1 mRNA by Forming a Protective RNA Duplex.** The results so far indicated that LEMD1-AS1 regulated LEMD1 mRNA expression levels. Consistent with this, the LEMD1 protein levels were also increased in OSC3 cells stably overexpressing LEMD1-AS1 and decreased in LEMD1-AS1-knockdown

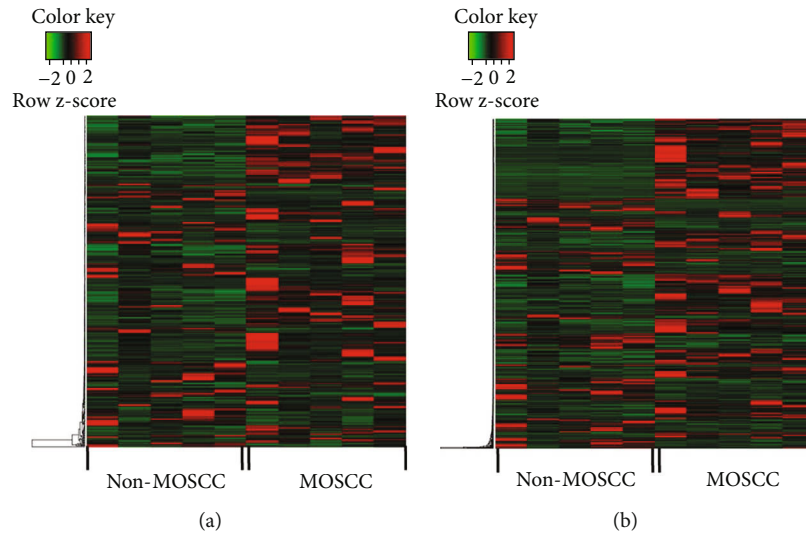


FIGURE 1: Heatmap of differentially expressed RNAs between metastatic OSCC and nonmetastatic OSCC. (a) mRNAs. (b) lncRNAs.

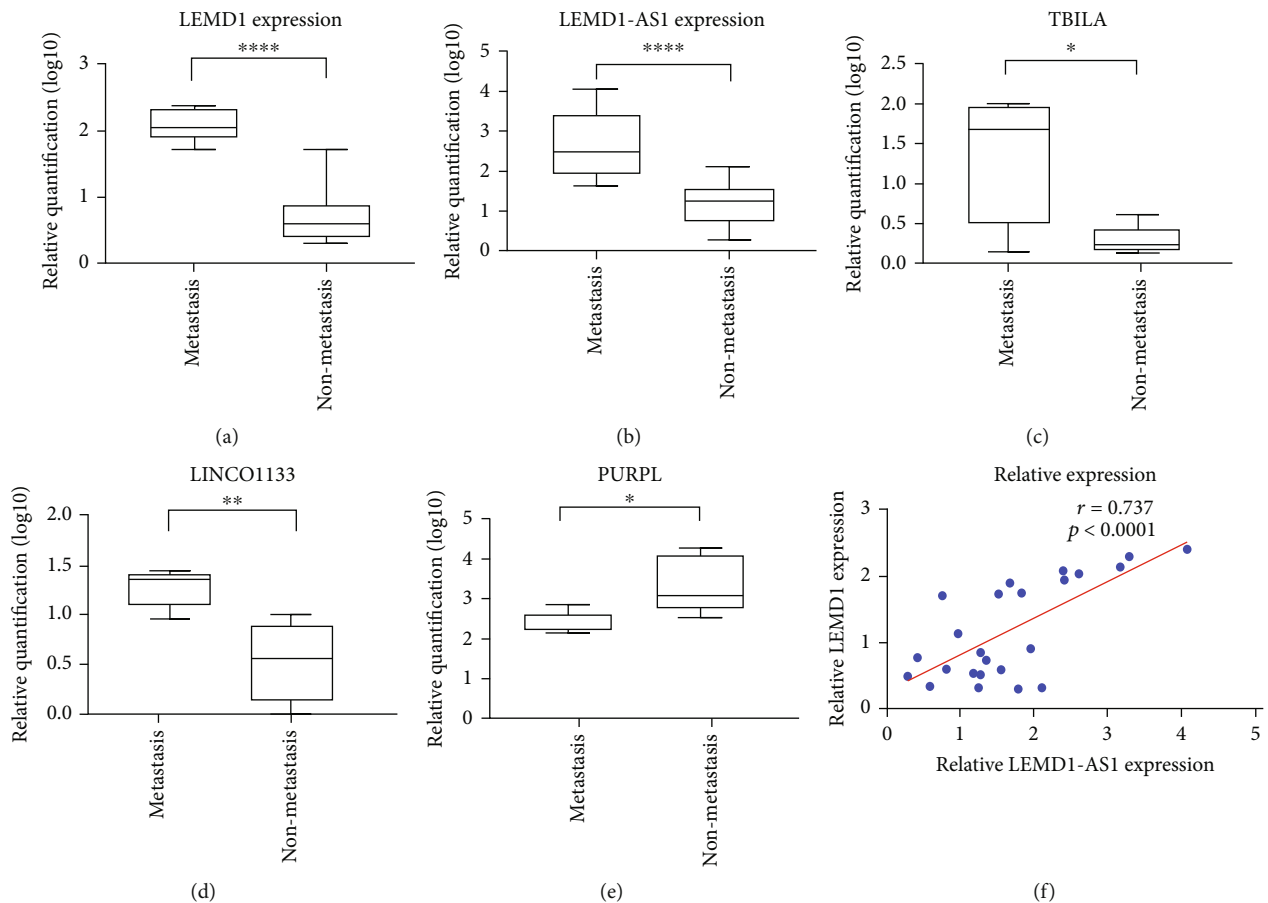
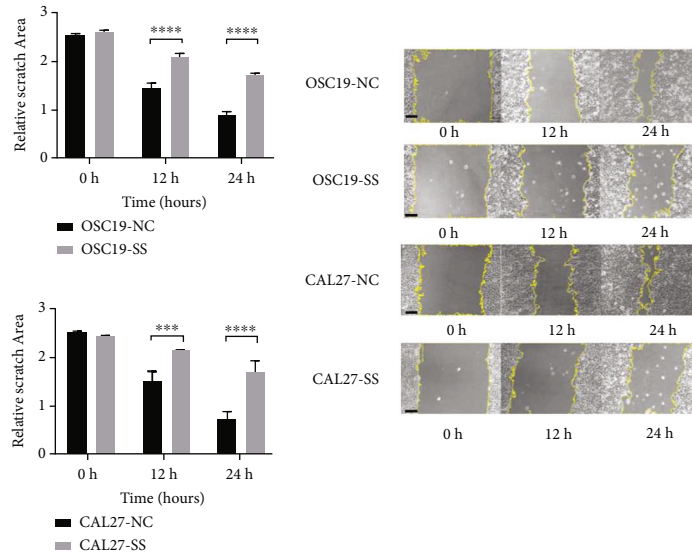


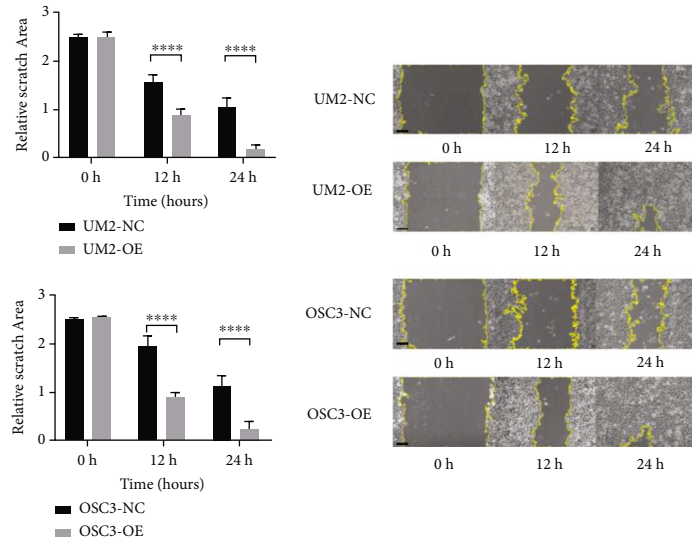
FIGURE 2: Validation of DERNAs expression level in 10 OSCC samples included in next generation sequencing. (a) LEMD1. (b) LEMD1-AS1. (c) TBILA. (d) LINC01133. (e) PURPL. (f) Correlation between LEMD1-AS1 and LEMD1 mRNA expression in 24 OSCC tissues. \* $P < 0.05$ ; \*\* $P < 0.01$ ; \*\*\* $P < 0.001$ ;  $P < 0.0001$ .

cells (Figure 5). LEMD1-AS1 is localized at the antisense chain of the LEMD1 gene. In addition, antisense lncRNAs increase the stability of their cognate sense mRNAs by form-

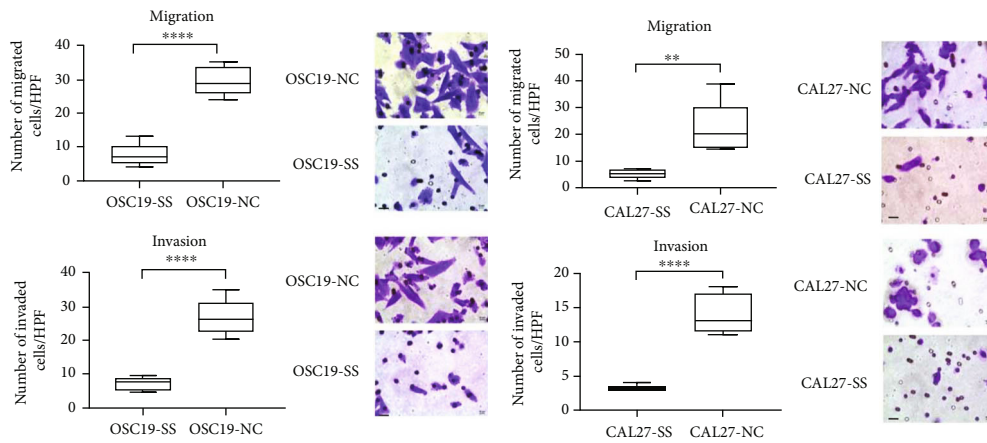
ing an RNA-RNA duplex, which also enhances the mRNA expression levels. Bioinformatics and gene sequence analysis revealed an overlapping (OL) region between LEMD1-AS1



(a)



(b)



(c)

FIGURE 3: Continued.

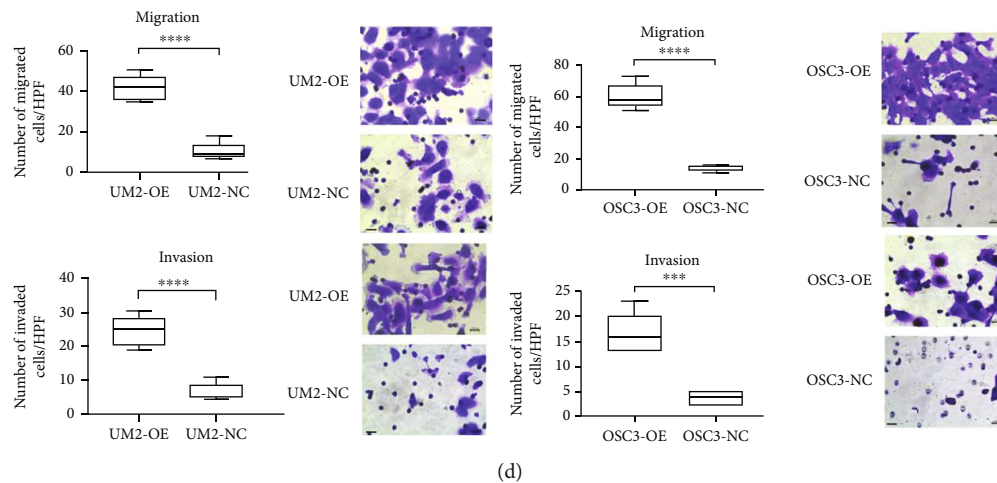


FIGURE 3: Wound healing assay showed that LEMD1-AS1 enhanced OSCC cells migration. The scope adumbrated by yellow line indicated the empty area calculated by ImageJ software. Data exhibited the mean of five biological replicates  $\pm$  SE. (a) Downregulating LEMD1-AS1 expression significantly inhibited cell migration and invasion in OSC19 and CAL27 cells. (b) Upregulating LEMD1-AS1 expression highly promoted migration and invasion of UM2 and OSC3. (c) Transwell assay showed that up-regulating LEMD1-AS1 stimulated migration and invasion ability, while silencing LEMD1-AS1 repressed. The effect of LEMD1-AS1 in OSC19 and CAL27(C), UM2 and OSC3 (d). SS: LEMD1-AS1 Smart Silencer; NC: normal control. OE: LEMD1-AS1-overexpressing. Scale bar in wound healing assay = 100  $\mu$ m. Scale bar in transwell assay = 20  $\mu$ m.

and LEMD1. The RNase protection assay further showed that the remnant of the OL region between LEMD1-AS1 and LEMD1 was higher than the non-OL region, indicating that the OL region was partially protected from RNase degradation (Figure 6(a)). These results indicated that the stability of LEMD1 mRNA was increased by LEMD1-AS1. To functionally validate this surmise, we treated control or LEMD1-AS1-overexpressing OSC3 cells with the RNA polymerase II inhibitor  $\alpha$ -amanitin to block new RNA synthesis and found that high levels of LEMD1-AS1 increased the stability of LEMD1 mRNA compared to that in control cells (Figure 6(b)). Thus, LEMD1-AS1 stabilizes and enhances the expression of LEMD1 mRNA in OSCC cells.

**2.7. LEMD1-AS1 Activates the PI3K-AKT Pathway.** On the basis of bioinformatics analysis and literature review, we analyzed the level of PI3K-AKT pathway-related proteins in the LEMD1-AS1-overexpressing OSCC cells. As shown in Additional Figure 8, p-PI3K and p-AKT were significantly upregulated in the OSC3 cells stably overexpressing LEMD1-AS1 compared to the control cells. Thus, LEMD1-AS1 might activate the PI3K-AKT pathway via increasing LEMD1 mRNA and protein levels.

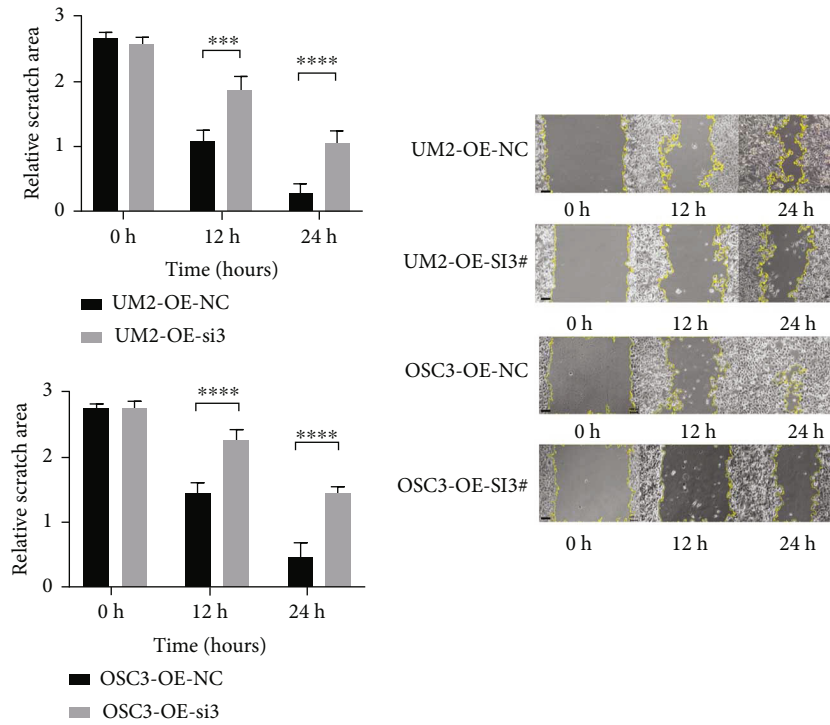
**2.8. LEMD1-AS1 Promoted Cervical LN and Hepatic Metastasis of OSCC In Vivo.** To confirm the biological function of LEMD1-AS1 *in vivo*, we established cervical LN and hepatic metastasis models in B/C mice. LEMD1-AS1-overexpressing (OSC3-OE) or normal control (OSC3-NC) OSCC cells were injected into the mice FOM, and while 37.5% of the OSC3-OE mice had cervical LN metastasis, the OSC3-NC group did not show any metastasis (Additional Figure 9). Contradictory to the *in vitro* results, the volume of the orthotopic tumor was markedly larger in the OSC3-OE

versus the OSC3-NC group, implying a greater proliferative capacity of the OSC3-OE cells *in vivo* (Figure 7).

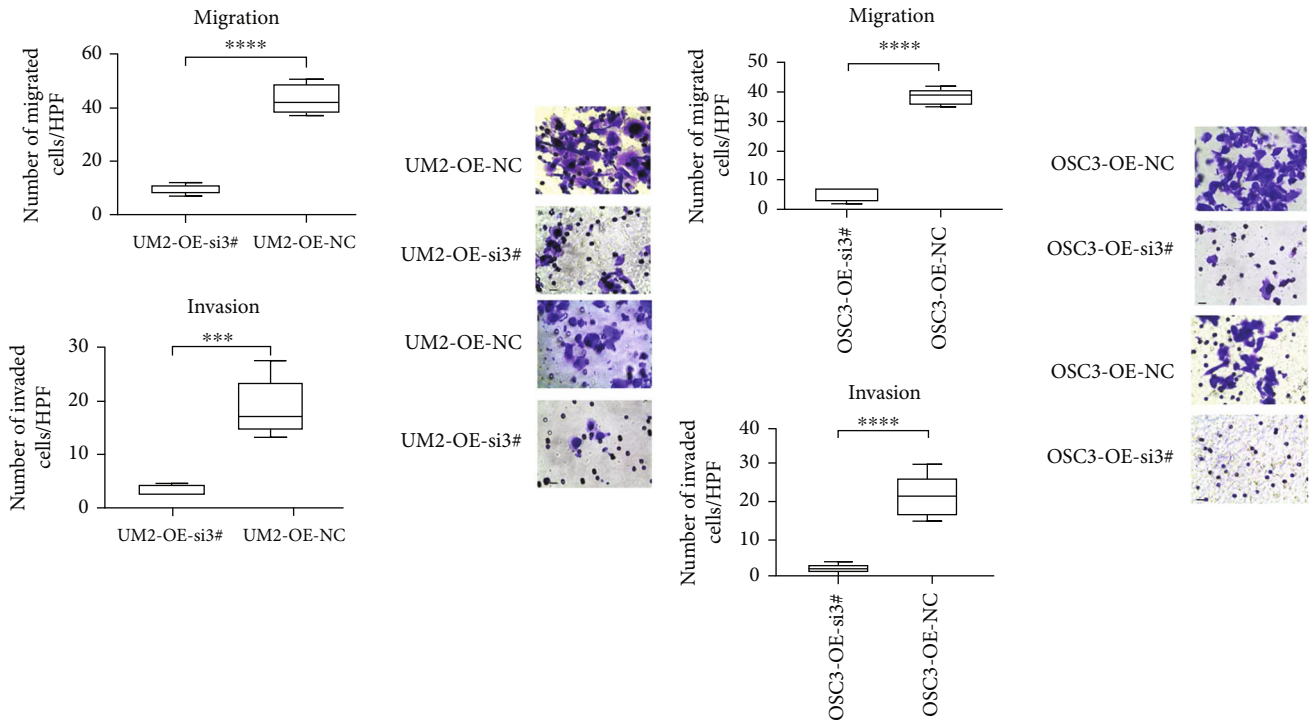
### 3. Discussion

Recent studies have associated aberrant expression levels of lncRNAs with OSCC genesis and progression. However, little is known regarding the function of dysregulated lncRNAs in OSCC with regional LN metastasis [13, 14], which is the most pervasive cause of death in OSCC patients. To determine the role of lncRNAs and their target genes in cervical LN metastasis of OSCC, we identified the differentially expressed mRNAs and lncRNAs between primary OSCC samples with and without regional LN metastasis, since the expression pattern of primary tissues was similar to that of metastatic tissues according to the single cell sequencing result of head and neck squamous cell carcinoma in 2017 [15]. The DERNA were enriched in GO components and KEGG pathways associated with tumor progression, migration and invasion, such as cell adhesion [16, 17], channel and receptor activity [18–20], cAMP signaling pathway [21], PI3K-AKT signaling pathway [22, 23], cytokine-cytokine receptor interaction, and CAMs [24]. The DELncRNA-DEmRNA network was subsequently constructed, and LEMD1-AS1 and its antisense mRNA LEMD1 were identified as a relevant pair in OSCC. LEMD1 [25] is a member of cancer-testis antigen (CTA) family and is located at chromosome 1q32.1. LEMD1-AS1 and LEMD1 were both upregulated in OSCC with LN metastasis compared to the nonmetastatic samples, indicating that LEMD1 and its reverse chain LEMD1-AS1 might enhance the migration and invasion abilities of OSCC cells.

Although LEMD1-AS1 gain/loss of function had no effect on OSCC cell growth, the LEMD1-AS1-overexpressing OSC3



(a)



(b)

FIGURE 4: Silencing LEMD1 could rescue the phenotype in stably expressing LEMD1-AS1 OSCC cells. Wound healing assay in UM2 cell and OSC3 cell (a). Transwell assay in UM2 cells and OSC3 cells (b). si3#: LEMD1-si3#; NC: normal-control-si; OE: LEMD1-AS1-overexpressing. Scale bar in wound healing assay = 100  $\mu$ m. Scale bar in transwell assay = 20  $\mu$ m.

cells resulted in larger tumors compared to the control cells. This was likely due to the fact that increased invasiveness of these cells led to impingement of the orthotopic tumor into the mandibula and FOM muscle, which resulted in larger

tumor volume. In the orthotopic OSCC model as well, OSC3-OE cells resulted in higher LN and hematogenous metastasis rates, which further verified the metastatic potential of LEMD1-AS1. Consistent with this, LEMD1-AS1

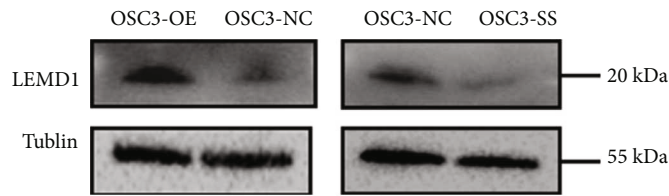


FIGURE 5: Western Blotting of LEMD1. After silencing LEMD1-AS1 for 48 hours in OSC3, the protein level of LEMD1 was diminished; and overexpression of LEMD1-AS1 increased LEMD1 expression at protein level. The samples were derived from the same experiment and that blots were processed in parallel. Full-length blots are presented in Supplementary Files.

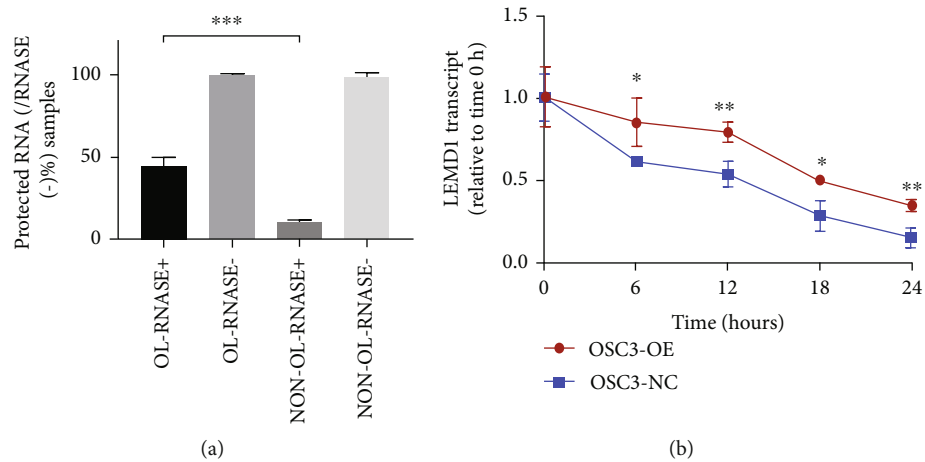


FIGURE 6: LEMD1-AS1 stabilized LEMD1 mRNA. (a) RNase protected assay indicated that the LEMD1-AS1 could protect OL region of LEMD1 from being depleted by RNase. (b) LEMD1-A1-overexpressing OSC3 cells were treated with 50  $\mu$ M  $\alpha$ -amanitin, and the LEMD1 mRNAs were detected by qPCR. High levels of LEMD1-AS1 increased the stability of LEMD1 mRNA compared to that in control cells. 18sRNA was applied as an internal control.

significantly promoted OSCC migration and invasion *in vitro*. Furthermore, LEMD1 silencing neutralized the pro-metastatic effects of LEMD1-AS1, indicating that LEMD1-AS1 directly targeted LEMD1 to increase OSCC cell invasiveness.

More than 63% of all transcripts in human cells possess antisense transcripts, which upon any perturbation can alter the expression of sense mRNAs [26–28]. Studies increasingly show that natural antisense lncRNA can stabilize its counterpart mRNA to increase its expression levels [29–31]. RNA-asRNA interactions are the result of the formation of RNA-RNA hybrid, partial physical binding [32, 33] or activating polysomes [27]. Bioinformatics analysis revealed that LEMD1-AS1 and LEMD1 formed a “tail-to-tail” pairing pattern with a 183 bp OL region. In addition, LEMD1-AS1 was localized in the cytoplasm, indicating the possibility of duplex formation between LEMD1 and its antisense lncRNA. Furthermore, the OL region on LEMD1 mRNA was protected from RNase digestion, which depleted most of the non-OL region. Finally, overexpression of LEMD1-AS1 increased stability of LEMD1 mRNA even in the presence of the RNA polymerase II inhibitor  $\alpha$ -amanitin. Thus, LEMD1-AS1 can stabilize LEMD1 mRNA and protect it from RNase via RNA-RNA interaction.

CTAs are upregulated in male germ cells and various cancer tissues, but not in normal tissues [34]. This protein cluster promotes epithelial mesenchymal transition (EMT)

[35] and metastasis [36], invasion, and carcinogenesis. Not surprisingly, CTAs are attractive diagnostic biomarkers and therapeutic targets in cancer. LEMD1 also promotes the initiation and progression of various cancers like colorectal cancer [25, 37, 38] and prostate cancer [39]. Sasahira et al. [40] identified LEMD1 as a novel oncogene in OSCC and supported its diagnostic and therapeutic potential. LEMD1 is also the target gene of microRNA-135 in anaplastic large cell lymphoma [41]. We have elucidated the regulatory interaction between LEMD1-AS1 and LEMD1 for the first time, which provides novel insights into the mechanism of CTAs in cancer.

The PI3K-AKT pathway is crucial for cancer initiation and progression, and is frequently disrupted in solid tumors [22, 42]. Mutation or alterations in the PI3K-AKT pathway have been identified in OSCC [24, 43–45]. Consistent with a previous study in gastric cancer [46], we found that the PI3K-AKT pathway was activated in OSC3 cells stably overexpressing LEMD1-AS1. We surmise therefore that LEMD1-AS1 upregulates LEMD1 to activate the PI3K-AKT pathway, which promotes OSCC migration and invasion.

Regional LN metastasis is the most common cause of the poor survival rate among OSCC patients. We identified 487 DE mRNAs and 1507 DELncRNAs in the metastatic versus nonmetastatic OSCC samples and characterized LEMD1-AS1/LEMD1 interaction as a promoter of OSCC metastasis

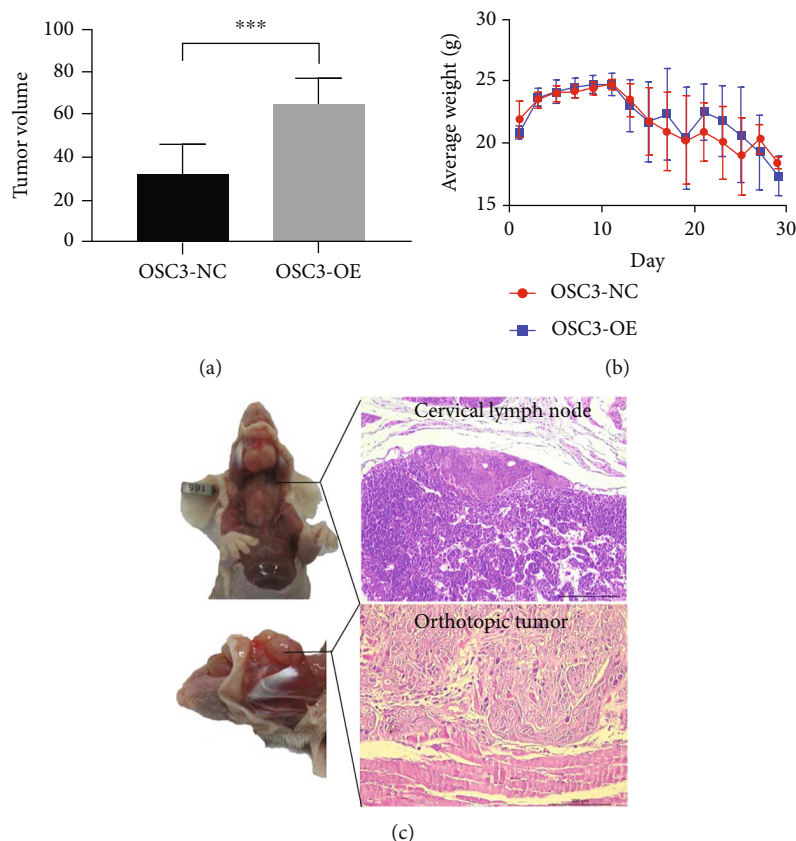


FIGURE 7: (a) The volume of the orthotopic tumor was markedly larger in the OSC3-OE compared to the OSC3-NC group. (b) However, there was no significant difference of weight between two groups. (c) Histochemical images of the orthotopic tumor and the metastatic lymph nodes.

for the first time. Mechanistically, LEMD1-AS1 activates the PI3K-AKT pathway by stabilizing and upregulating LEMD1. However, survival analysis related to LEMD1-AS1 expression was not possible due to the short follow-up time. In addition, the exact regulatory axis between LEMD1-AS1, LEMD1, and PI3K-AKT pathway in OSCC progression remains to be elucidated. Besides, the targeted genes of LEMD1-AS1 might not be only LEMD1; the relationship between its targeted genes should be further investigated. Our findings have to be validated on larger cohorts with longer follow-up.

#### 4. Conclusions

LEMD1-AS1 was substantially increased in metastatic OSCC tissues and cell lines and promoted OSCC migration and invasion *in vitro* and *in vivo* by stabilizing its antisense transcript LEMD1, which is a potential activator of the PI3K-AKT signaling pathway. Therefore, LEMD1-AS1 is a novel diagnostic biomarker and immunotherapeutic target for metastatic OSCC.

#### 5. Methods

**5.1. Human Tissue Samples.** Tumor tissues were collected from OSCC patients who underwent surgery at the Xiangya Hospital of Central South University. The patients that

received radiotherapy or chemotherapy prior to the surgery were excluded. The baseline data of recruited patients is present in Table 1. All primary tumor tissue samples were confirmed by two experienced pathologists and stored at  $-80^{\circ}\text{C}$  for RNA extraction. The clinical characteristics of the included patients were also recorded. The informed consent was obtained from all subjects. This study was approved by the ethics committee of the Xiangya Hospital (No. 201907790).

**5.2. Next-Generation RNA Sequencing and Bioinformatics Analysis.** Total RNA was isolated from 5 patients with cervical LN metastasis and 5 patients without cervical LN metastasis using the TRIzol reagent (Invitrogen, CA, USA) according to the manufacturer's instructions. The quality of RNA was evaluated by Qubit, Nanodrop, and Agilent 2100 Bioanalyzer. RNA sequencing libraries were prepared using TruSeq Stranded Total RNA Library Prep Kit according to manufacturer's specifications. The rRNAs were then removed, and the remaining transcripts were purified and fragmented. First-strand cDNA synthesis was performed using random primers, followed by second-strand cDNA synthesis and end repair. The 3' ends of the cDNAs were adenylated and ligated to Illumina Truseq adaptors for PCR. The cDNA libraries were sequenced by Illumina Hiseq 2500. All bioinformatical analysis were performed by R and



TABLE 1: Baseline data of the patients recruited.

No.	Gender	Age (year)	Location	TNM stage	Differentiation level	Drinking	Smoking (n/day)
1	Male	52	Tongue	T1N2M0	High	+	10-20
2	Male	29	Tongue	T1N2M0	Moderate-high	—	<5
3	Male	50	Tongue	T1N1M0	High	+	0
4	Male	39	Bucal	T1N1M0	Moderate-high	+	10-20
5	Male	48	Tongue	T1N1M0	High	+	0
6	Male	52	Buccal mucosa	T3N0M0	High	—	10-20
7	Male	65	Tongue	T3N0M0	High	+	10-20
8	Male	47	Buccal mucosa	T3N0M0	High	+	10-20
9	Male	55	Buccal mucosa	T3N0M0	Moderate-high	—	<5
10	Male	55	Tongue	T3N0M0	High	+	<5

TABLE 2: Primers used for qRT-PCR.

Gene	Forward primer	Reverse primer
LEMD1-AS1	TGCAGCTCAGTCAGACCAAA	AGGCAGACGTGGGAGGAT
LEMD1	GAGACCAAGCACCAGAATCA	ACCAAGCACAGCAAGCTTCA
LEMD1-OL	TGGACCCAGAGAGCTGGATG	TGCGTTTAGTGGTGAAGCC
LEMD1-non-OL	ACTTCTATCATCATGGTGGATG	GATCTGTGAGAGCAGCACAG
GAPDH	AGTGGTCGTTGAGGGCAAT	GCATCCTGGGCTACACTGAG
18sRNA	GTAACCCGTTGAACCCCAT	CCATCCAATCGGTAGTAGCG
PURPL	GGCATGATCTCGGCTCACTA	CAGATCACGAGGTCAGGAGA
TBILA	TGACTTTCAAAGCACAGGAGG	CCATGATTCTGTCCCAGAGA
LINC01133	TGGTATTTTCATCATTGTGGTGT	TCAGGGTAGTGTTTTGGTCTTT

LncTar software. *P* value was adjusted for multiple testing adopting the false discovery rate method, and  $|\log_2 \text{fold change (FC)}| > 1.0$  and *P* value < 0.05 were set as the cutoff criteria.

**5.3. OSCC Cell Lines and Animals.** OSCC cell lines including UM1, UM2, OSC3, OSC19, and CAL27 were cultured in high-glucose DMEM (Gibco, CA, USA) supplemented with 10% fetal bovine serum (Gibco, CA, USA), 100 U/ml penicillin, and 100 mg/ml streptomycin (Gibco, CA, USA) at 37% in a humidified incubator containing 5% CO<sub>2</sub>. BALB/c-nude mice (5-week-old) were obtained from the Experiment Animal Center of Central South University. All animal experiments were approved by the Institutional Animal Care Committee of Central South University (No.2019sydw0116).

**5.4. qRT-PCR Analysis.** Total RNA was isolated using TRIzol reagent (Invitrogen, CA, USA) as described above, and reverse transcribed to cDNA by HiScript III RT SuperMix (Vazyme, Nanjing, China). Real-time PCR was performed on QuaintStudio 7 Flex System (Thermo Fisher, CA, USA) using the SYBR All-in-One qPCR mix (GeneCopoeia, Guangzhou, China), and relative gene expression was calculated using  $2^{-\Delta\Delta CT}$  method normalized to that of GAPDH or 18sRNA. Primer sequences are listed in Table 2.

**5.5. Fluorescent in Situ Hybridization.** RNA fluorescence in situ hybridization (RNA-FISH) was performed using a FISH

TABLE 3: Sequences of Smart Silencer for LEMD1-AS1 and siRNA for LEMD1.

Name	Targeted Sequence (5'-3')
LEMD1-AS1 Smart Silencer	GACCAAACCTCTCTGAATA
	GACAGAACAAGAAGCACAA
	CTCTACATATCCATCACAT
	TCCAGCGCCACTTTCTCAG
	GTCAGGACACAACAATAGAG
ACAGCTCCTAGGCAATCAAA	
LEMD1-siRNA1#	GAATCACATATGGGACTAT
LEMD1-siRNA2#	CGGAAGACCAGACTATCGA
LEMD1-siRNA3#	GCTGGAGAGAAGAAGGTTT

kit (Ribobio, Guangzhou, China) according to the manufacturer's instruction. Briefly, the suitably treated cells were fixed with 4% formaldehyde for 10 min, permeabilized with 0.5% Triton X-100 in PBS, and subsequently blocked through prehybridization at 37°C for 30 minutes. The cells were then incubated overnight with 50 nM FISH probe (Ribobio Co.) in 100  $\mu$ l hybridization buffer at 37°C. The slides were washed with a gradient of hybridization wash buffer (4  $\times$  SCC with 0.1% Tween-20, 2  $\times$  SCC, 1  $\times$  SCC) at 42°C for 5 min, respectively, and air-dried. After counterstaining with 4',6-diamidino-2-phenylindole (DAPI), the slides were imaged under a fluorescence microscope.

**5.6. Transfection.** The Ribo™ Smart Silencer targeting LEMD1-AS1 was obtained from RiboBio (Guangzhou, China) and included three siRNA and three antisense oligonucleotides targeting different sequences. The siRNAs for human LEMD1 were designed and synthesized by RiboBio (China). Cells were transfected with the respective siRNAs using Lipofectamine3000 Reagent (Invitrogen, CA, USA). In addition, OSCC cells were transduced with LEMD1-AS1 expressing lentivirus (GENECHEM, Shanghai, China) with specific MOI (multiplicity of infection). The siRNA sequences are listed in Table 3.

**5.7. CCK-8 Assay.** Cell growth was monitored using the 2-(2-methoxy-4-nitrophenyl)-3-(4-nitrophenyl)-5-(2,4-disulfothenyl)-2H-tetrazolium reagent (CCK-8, Meilunbio, Dalian, China) assay according to manufacturer's instruction. The transient and stable transfectants were seeded in 96-well plates at the density of 3000 cells/well with 5 replicates per sample. CCK-8 reagent was added to each well after 1, 2, and 3 days of culture, and the absorbance of each well was measured at 450 nm.

**5.8. Wound Healing Assay.** Suitably treated cells were seeded in six-well plates and grown till confluency. The monolayer was scratched across the plate using a sterile 10  $\mu$ l pipette tip, and the dislodged cells were washed. The wounded regions were photographed at 0, 12, and 24 hours after scratching, and the scratch area was calculated by ImageJ software.

**5.9. Transwell Assay.** Cells harvested 36–48 hours after transient or stable transfection were seeded into the upper chambers of a transwell insert (Corning (3422, 354480), NY, USA) at the density of  $8 \times 10^4$  cells/well in 200  $\mu$ l serum-free high-glucose DMEM. The lower chambers were filled with 400  $\mu$ l DMEM supplemented with 20% FBS. After a 24h culture, the migrated cells were fixed with 4% paraformaldehyde for 30 minutes, stained with crystal violet for 30 minutes, and counted.

**5.10. Western Blotting.** Protein was extracted by lysing the cells in RIPA buffer (Abcam, NY, USA) supplemented with protease inhibitors and phosphate inhibitors, separated by SDS-PAGE and transferred onto a PVDF membrane. After blocking in 5% skimmed milk for 1 hour, the gels were incubated overnight with the primary antibodies (Abcam, MA, USA and CST, MA, USA), followed by the HRP-conjugated IgG secondary antibody. The bands were visualized using ECL Substrates (SAB, MD, USA). Tubulin was used as the loading control.

**5.11. RNase Protection Assay.** RNA duplex formation between LEMD1-AS1 and LEMD1 was assessed with the RNase A+T cocktail (Invitrogen, CA, USA) that can only digest single-stranded and not duplex RNAs. Briefly, the samples were incubated with the enzyme cocktail at 37°C for 30 minutes, and the remaining double-stranded RNA was extracted using RNeasy Kit (Tianmo, Beijing, China) and analyzed by qRT-PCR.

**5.12. Stability and  $\alpha$ -Amanitin Treatment.** OSC3 cells stably expressing LEMD1-AS1 or the empty vector were seeded into 6-well plates and treated with 50  $\mu$ M of the RNA synthesis blocker  $\alpha$ -amanitin. The cells were harvested 0, 6, 12, 18, and 24 hours posttreatment and analyzed by qRT-PCR. The 18s RNA was used as the internal control since it is stable after  $\alpha$ -amanitin treatment.

**5.13. Animal Experiments.** An orthotopic oral tumor model was established in mice by injecting control or LEMD1-AS1-overexpressing  $2 \times 10^5$  OSC3 cells ( $n=8$  per group) in 100  $\mu$ l DMEM into the floor of mouth (FOM) via submental to the space between the FOM muscles (around 5 mm). The mice were sacrificed on day 30 after implantation or when their weight was reduced to 16 grams (g) or less. The tongue and cervical LNs were collected and fixed in 10% paraformaldehyde immediately for HE staining. The volume of the orthotopic tumor was calculated as  $\text{length} \times \text{width}^2/2$ . All tissue staining results were examined by two expert pathologists.

**5.14. Statistical Analysis.** All data were analyzed using the SPSS 22.0 statistical software package (SPSS Inc., Chicago, IL, USA) and visualized with Graphpad Prism 7. The results were expressed as the mean  $\pm$  SD of three experiments. Two or multiple groups were compared using two-tailed Student's *t*-test and One-way ANOVA, respectively. Pearson's correlation coefficient was used to analyze the correlation between LEMD1-AS1 and LEMD1 expression levels. *P* value < 0.05 was considered statistically significant.

## Data Availability

The data used to support the findings of this study are included within the article and the supplementary information files.

## Ethical Approval

This study was approved by the Ethics Committee of the Xiangya Hospital (No. 201907790) and the Institutional Animal Care Committee of Central South University (No. 2019sydw0116).

## Consent

The informed consent was obtained from all subjects. All methods were carried out in accordance with relevant guidelines and regulations (for both humans and animals).

## Conflicts of Interest

The authors declare that they have no competing interests.

## Authors' Contributions

Zaiye Li and Canhua Jiang did the conceptualization. Zaiye Li is assigned to the methodology. Zaiye Li is assigned to the software. Ning Li and Jianjun Wu did the validation. Jie Wang did the formal analysis and investigation. Jianjun Wu is assigned to the resources. Zaiye Li, Jianjun Wu and

Canhua Jiang curated the data. Zaiye Li and Jie Wang did the writing—original draft preparation. Jie Wang and Canhua Jiang did the writing—review and editing. Jianjun Wu worked on visualization. Jie Wang and Canhua Jiang worked on supervision. Canhua Jiang is responsible for the project administration. Canhua Jiang and Zaiye Li acquired funding. All authors have read and agreed to the published version of the manuscript.

## Acknowledgments

This study was supported by the Natural Science Foundation of Hunan Province, China (Grant No. 2020JJ4881), and the Fundamental Research Funds for Central Universities of the Central South University (2019zzts795).

## Supplementary Materials

Additional Figure 1: functional enrichment analysis of DErnRNAs. (A) The bar plot of GO analyses. Purple for MF, orange for CC, and yellow for BP. (B) The top 10 enrichment scores in KEGG pathway. Additional Figure 2: DElncRNA-DErnRNA interaction network in *cis*- and *trans*-way. Circles indicate mRNAs, and rectangles indicate lncRNAs. Red nodes mean upregulation in metastatic OSCC samples, while green nodes represent downregulation. (A) *Cis*-way. (B) *Trans*-way. Additional Figure 3: expression of LEMD1-AS1 in OSCC cell lines. Five OSCC cell lines were examined. The metastatic OSCC cell lines UM1, OSC19, and CAL27 showed significantly higher LEMD-AS1 levels compared to the nonmetastatic UM2 and OSC3 cells. The red \* indicated statistical difference with OSC3, and blue one indicated that with UM1. Additional Figure 4: subcellular location of LEMD1-AS1. Fish assay revealed that LEMD1-AS1 mainly is located in the cytoplasm, while a few in the nucleus. Red shows LEMD1-AS1, and blue shows nucleus; scale bar = 50  $\mu$ m. Additional Figure 5: expression of LEMD1AS1 and LEMD1 in transfectants. (A) LEMD1-AS1 knockdown efficiency in OSC19 and CAL27 with Smart Silencer. (B) LEMD1-AS1 overexpression efficiency in UM2 and OSC3 with lentivirus. (C) LEMD1 mRNA expression level was decreased in LEMD1-AS1-knockdown OSCC cells. (D) LEMD1 mRNA expression level was elevated in LEMD1-AS1-overexpressing OSCC cells. Additional Figure 6: CCK8 assay implied that LEMD1-AS1 was not able to influence the cell growth in OSCC cells. (A) Knockdown of LEMD1-AS1 in OSC19 and CAL27 cells did not affect cell growth. (B) Overexpression of LEMD1-AS1 in UM2 and OSC3 cells did not change the ability of growth. SS: LEMD1-AS1 Smart Silencer; NC: normal control; OE: LEMD1-AS1-overexpressing. Additional Figure 7: apply 3 sequences of siRNA to inhibit LEMD1 expression. Among these, si3# had the highest transfection efficiency. Additional Figure 8: Western Blotting showed that the level of PI3K-AKT pathway-related proteins was increased in LEMD1-AS1-overexpressing OSC3 cells compared to the control cells. Additional Figure 9: the metastasis ratio of two groups (LEM1-AS1-overexpressing and normal control (NC)). (Supplementary Materials)

## References

- [1] R. L. Siegel, K. D. Miller, and A. Jemal, "Cancer statistics, 2019," *CA: a cancer journal for clinicians*, vol. 69, no. 1, pp. 7–34, 2019.
- [2] M. Du, R. Nair, L. Jamieson, Z. Liu, and P. Bi, "Incidence trends of lip, oral cavity, and pharyngeal cancers: global burden of disease 1990-2017," *Journal of dental research*, vol. 99, no. 2, pp. 143–151, 2020.
- [3] R. L. Siegel, K. D. Miller, H. E. Fuchs, and A. Jemal, "Cancer statistics, 2021," *CA: a cancer journal for clinicians*, vol. 71, no. 1, pp. 7–33, 2021.
- [4] S. Warnakulasuriya, "Global epidemiology of oral and oropharyngeal cancer," *Oral oncology*, vol. 45, no. 4-5, pp. 309–316, 2009.
- [5] C. Rivera and B. Venegas, "Histological and molecular aspects of oral squamous cell carcinoma (review)," *Oncology letters*, vol. 8, no. 1, pp. 7–11, 2014.
- [6] C. P. Ponting, P. L. Oliver, and W. Reik, "Evolution and functions of long noncoding RNAs," *Cell*, vol. 136, no. 4, pp. 629–641, 2009.
- [7] J. S. Mattick and J. L. Rinn, "Discovery and annotation of long noncoding RNAs," *Nature structural & molecular biology*, vol. 22, no. 1, pp. 5–7, 2015.
- [8] X. Luo, Y. Qiu, Y. Jiang et al., "Long non-coding RNA implicated in the invasion and metastasis of head and neck cancer: possible function and mechanisms," *Molecular cancer*, vol. 17, no. 1, p. 14, 2018.
- [9] S. Ghafouri-Fard, H. Mohammad-Rahimi, M. Jazaeri, and M. Taheri, "Expression and function of long non-coding RNAs in head and neck squamous cell carcinoma," *Experimental and Molecular Pathology*, vol. 112, article 104353, 2020.
- [10] M. Guttman and J. L. Rinn, "Modular regulatory principles of large non-coding RNAs," *Nature*, vol. 482, no. 7385, pp. 339–346, 2012.
- [11] Y. Zhao, Y. Liu, L. Lin et al., "The lncRNA MACC1-AS1 promotes gastric cancer cell metabolic plasticity via AMPK/Lin28 mediated mRNA stability of MACC1," *Molecular cancer*, vol. 17, no. 1, p. 69, 2018.
- [12] Z. Zhang, Z. Peng, J. Cao et al., "Long noncoding RNA PXN-AS1-L promotes non-small cell lung cancer progression via regulating PXN," *Cancer cell international*, vol. 19, no. 1, p. 20, 2019.
- [13] Y. Wang, X. Zhang, Z. Wang et al., "LncRNA-p23154 promotes the invasion-metastasis potential of oral squamous cell carcinoma by regulating Glut1-mediated glycolysis," *Cancer letters*, vol. 434, pp. 172–183, 2018.
- [14] Y. L. Qiu, Y. H. Liu, J. D. Ban et al., "Pathway analysis of a genome-wide association study on a long non-coding RNA expression profile in oral squamous cell carcinoma," *Oncology reports*, vol. 41, no. 2, pp. 895–907, 2019.
- [15] S. V. Puram, I. Tirosh, A. S. Parkh et al., "Single-cell transcriptomic analysis of primary and metastatic tumor ecosystems in head and neck cancer," *Cell*, vol. 171, no. 7, pp. 1611–24.e24, 2017.
- [16] E. Bonastre, E. Brambilla, and M. Sanchez-Cespedes, "Cell adhesion and polarity in squamous cell carcinoma of the lung," *The Journal of pathology*, vol. 238, no. 5, pp. 606–616, 2016.
- [17] F. Ramadan, A. Fahs, S. E. Ghayad, and R. Saab, "Signaling pathways in rhabdomyosarcoma invasion and metastasis," *Cancer Metastasis Reviews*, vol. 39, no. 1, pp. 287–301, 2020.

- [18] H. Wang, L. Zou, K. Ma et al., "Cell-specific mechanisms of TMEM16A  $\text{Ca}^{2+}$ -activated chloride channel in cancer," *Molecular cancer*, vol. 16, no. 1, p. 152, 2017.
- [19] N. Deliot and B. Constantin, "Plasma membrane calcium channels in cancer: alterations and consequences for cell proliferation and migration," *Biochimica et Biophysica Acta*, vol. 1848, no. 10, pp. 2512–2522, 2015.
- [20] C. S. Hinrichs, "Molecular pathways: breaking the epithelial cancer barrier for chimeric antigen receptor and T-cell receptor gene therapy," *Clinical cancer research : an official journal of the American Association for Cancer Research*, vol. 22, no. 7, pp. 1559–1564, 2016.
- [21] J. Li, M. A. Duran, N. Dhanota et al., "Metastasis and immune evasion from extracellular cGAMP hydrolysis," *Cancer Discovery*, vol. 11, no. 5, pp. 1212–1227, 2021.
- [22] D. Tewari, P. Patni, A. Bishayee, A. N. Sah, and A. Bishayee, "Natural products targeting the PI3K-Akt-mTOR signaling pathway in cancer: a novel therapeutic strategy," *Seminars in cancer biology*, 2019.
- [23] B. Yang, L. Li, G. Tong et al., "Circular RNA circ\_001422 promotes the progression and metastasis of osteosarcoma via the miR-195-5p/FGF2/PI3K/Akt axis," *Journal of Experimental & Clinical Cancer Research*, vol. 40, no. 1, p. 235, 2021.
- [24] Z. Li, C. Jiang, and Y. Yuan, "TCGA based integrated genomic analyses of ceRNA network and novel subtypes revealing potential biomarkers for the prognosis and target therapy of tongue squamous cell carcinoma," *PLoS One*, vol. 14, no. 5, article e0216834, 2019.
- [25] D. Yuki, Y. M. Lin, Y. Fujii, Y. Nakamura, and Y. Furukawa, "Isolation of LEM domain-containing 1, a novel testis-specific gene expressed in colorectal cancers," *Oncology reports*, vol. 12, no. 2, pp. 275–280, 2004.
- [26] S. Katayama, Y. Tomaru, T. Kasukawa et al., "Antisense transcription in the mammalian transcriptome," *Science*, vol. 309, no. 5740, pp. 1564–1566, 2005.
- [27] C. Carrieri, L. Cimatti, M. Biagioli et al., "Long non-coding antisense RNA controls *Uchl1* translation through an embedded SINEB2 repeat," *Nature*, vol. 491, no. 7424, pp. 454–457, 2012.
- [28] R. Yelin, D. Dahary, R. Sorek et al., "Widespread occurrence of antisense transcription in the human genome," *Nature biotechnology*, vol. 21, no. 4, pp. 379–386, 2003.
- [29] K. Matsui, M. Nishizawa, T. Ozaki et al., "Natural antisense transcript stabilizes inducible nitric oxide synthase messenger RNA in rat hepatocytes," *Hepatology*, vol. 47, no. 2, pp. 686–697, 2008.
- [30] C. L. Zhang, K. P. Zhu, and X. L. Ma, "Antisense lncRNA FOXC2-AS1 promotes doxorubicin resistance in osteosarcoma by increasing the expression of FOXC2," *Cancer letters*, vol. 396, pp. 66–75, 2017.
- [31] B. Huang, J. H. Song, Y. Cheng et al., "Long non-coding antisense RNA KRT7-AS is activated in gastric cancers and supports cancer cell progression by increasing KRT7 expression," *Oncogene*, vol. 35, no. 37, pp. 4927–4936, 2016.
- [32] G. Gao, W. Li, S. Liu et al., "The positive feedback loop between ILF3 and lncRNA ILF3-AS1 promotes melanoma proliferation, migration, and invasion," *Cancer management and research*, vol. Volume 10, pp. 6791–6802, 2018.
- [33] J. Sun, X. Wang, C. Fu et al., "Long noncoding RNA FGFR3-AS1 promotes osteosarcoma growth through regulating its natural antisense transcript FGFR3," *Molecular biology reports*, vol. 43, no. 5, pp. 427–436, 2016.
- [34] M. J. Scanlan, A. O. Gure, A. A. Jungbluth, L. J. Old, and Y. T. Chen, "Cancer/testis antigens: an expanding family of targets for cancer immunotherapy," *Immunological Reviews*, vol. 188, no. 1, pp. 22–32, 2002.
- [35] P. Yang, Z. Huo, H. Liao, and Q. Zhou, "Cancer/testis antigens trigger epithelial-mesenchymal transition and genesis of cancer stem-like cells," *Current pharmaceutical design*, vol. 21, no. 10, pp. 1292–1300, 2015.
- [36] B. Shang, A. Gao, Y. Pan et al., "CT45A1 acts as a new proto-oncogene to trigger tumorigenesis and cancer metastasis," *Cell death & disease*, vol. 5, no. 6, article e1285, 2014.
- [37] R. Takeda, Y. Hirohashi, M. Shen et al., "Identification and functional analysis of variants of a cancer/testis antigen LEMD1 in colorectal cancer stem-like cells," *Biochemical and biophysical research communications*, vol. 485, no. 3, pp. 651–657, 2017.
- [38] D. Li, D. Wang, H. Liu, and X. Jiang, "LEM domain containing 1 (LEMD1) transcriptionally activated by SRY-related high-mobility-group box 4 (SOX4) accelerates the progression of colon cancer by upregulating phosphatidylinositol 3-kinase (PI3K)/protein kinase B (Akt) signaling pathway," *Bioengineered*, vol. 13, no. 4, pp. 8087–8100, 2022.
- [39] S. Ghafouri-Fard, Z. Ousati Ashtiani, B. Sabah Golian, S. M. Hasheminasab, and M. H. Modarressi, "Expression of two testis-specific genes, SPATA19 and LEMD1, in prostate cancer," *Archives of Medical Research*, vol. 41, no. 3, pp. 195–200, 2010.
- [40] T. Sasahira, M. Kurihara, C. Nakashima, T. Kirita, and H. Kuniyasu, "LEM domain containing 1 promotes oral squamous cell carcinoma invasion and endothelial transmigration," *British journal of cancer*, vol. 115, no. 1, pp. 52–58, 2016.
- [41] H. Matsuyama, H. I. Suzuki, H. Nishimori et al., "miR-135b mediates NPM-ALK-driven oncogenicity and renders IL-17-producing immunophenotype to anaplastic large cell lymphoma," *Blood*, vol. 118, no. 26, pp. 6881–6892, 2011.
- [42] J. A. Engelman, J. Luo, and L. C. Cantley, "The evolution of phosphatidylinositol 3-kinases as regulators of growth and metabolism," *Nature reviews Genetics*, vol. 7, no. 8, pp. 606–619, 2006.
- [43] D. R. Simpson, L. K. Mell, and E. E. Cohen, "Targeting the PI3K/AKT/mTOR pathway in squamous cell carcinoma of the head and neck," *Oral oncology*, vol. 51, no. 4, pp. 291–298, 2015.
- [44] R. Vander Broek, S. Mohan, D. F. Eytan, Z. Chen, and C. Van Waes, "The PI3K/Akt/mTOR axis in head and neck cancer: functions, aberrations, cross-talk, and therapies," *Oral diseases*, vol. 21, no. 7, pp. 815–825, 2015.
- [45] F. E. Marquard and M. Jucker, "PI3K/AKT/mTOR signaling as a molecular target in head and neck cancer," *Biochemical Pharmacology*, vol. 172, article 113729, 2020.
- [46] Q. Li, Y. Ge, X. Chen et al., "LEM domain containing 1 promotes proliferation via activating the PI3K/Akt signaling pathway in gastric cancer," *Journal of Cellular Biochemistry*, vol. 120, no. 9, pp. 15190–15201, 2019.